



Published in final edited form as:

Dev Biol. 2017 June 01; 426(1): 43–55. doi:10.1016/j.ydbio.2017.04.008.

Genetic dissection of the planarian reproductive system through characterization of *Schmidtea mediterranea* CPEB homologs

Labib Rouhana^{a,b,*}, Junichi Tasaki^a, Amir Saberi^{b,1}, and Phillip A. Newmark^{b,2}

^aDepartment of Biological Sciences, Wright State University, 3640 Colonel Glenn Highway, Dayton, OH 45435, USA

^bHoward Hughes Medical Institute and Department of Cell and Developmental Biology, University of Illinois at Urbana-Champaign, 601 S. Goodwin Ave., Urbana, IL 61801, USA

Abstract

Cytoplasmic polyadenylation is a mechanism of mRNA regulation prevalent in metazoan germ cells; it is largely dependent on Cytoplasmic Polyadenylation Element Binding proteins (CPEBs). Two CPEB homologs were identified in the planarian *Schmidtea mediterranea*. *Smed-CPEB1* is expressed in ovaries and yolk glands of sexually mature planarians, and required for oocyte and yolk gland development. In contrast, *Smed-CPEB2* is expressed in the testes and the central nervous system; its function is required for spermatogenesis as well as non-autonomously for development of ovaries and accessory reproductive organs. Transcriptome analysis of CPEB knockdown animals uncovered a comprehensive collection of molecular markers for reproductive structures in *S. mediterranea*, including ovaries, testes, yolk glands, and the copulatory apparatus. Analysis by RNA interference revealed contributions for a dozen of these genes during oogenesis, spermatogenesis, or capsule formation. We also present evidence suggesting that *Smed-CPEB2* promotes translation of Neuropeptide Y-8, a prohormone required for planarian sexual maturation. These findings provide mechanistic insight into potentially conserved processes of germ cell development, as well as events involved in capsule deposition by flatworms.

This is an open access article under the CC BY-NC-ND license.

*Corresponding author at: Department of Biological Sciences, Wright State University, 3640 Colonel Glenn Highway, Dayton, OH 45435, USA labib.rouhana@wright.edu (L. Rouhana).

¹Current address: Johns Hopkins University School of Medicine, Baltimore, MD 21205, USA.

²Current address: Morgridge Institute for Research, Department of Zoology, University of Wisconsin–Madison, Madison, WI 53715, USA.

Appendix A. Supporting information

Supplementary data associated with this article can be found in the online version at doi:10.1016/j.ydbio.2017.04.008.

Competing interests

The authors declare no competing interests.

Author contributions

LR conceived this study, analyzed the data and wrote the manuscript. Experiments were performed by LR, AS and JT. PAN participated in the study's design and manuscript preparation.

Data availability

GenBank accession number KY847525-KY847539 and NCBI BioProject accession number PRJNA319057 (www.ncbi.nlm.nih.gov/bioproject/319057).

Keywords

CPEB; Spermatogenesis; Oogenesis; Vitellaria; Ectolecithal reproduction; Platyhelminthes

1. Introduction

Sexual reproduction relies on assembly of functional gametes, as well as on processes that bring these together and support embryonic development. Genetic screens performed using invertebrate model organisms, such as *Drosophila melanogaster* and *Caenorhabditis elegans*, have revealed conserved genetic pathways that drive sexual reproduction. Molecular mechanisms for chromatin modification, mRNA regulation, and extrinsic signaling, have emerged from such studies as unifying themes in metazoan germline development (Kimble, 2011; Kimmins and Sassone-Corsi, 2005; Sasaki and Matsui, 2008; Seydoux and Braun, 2006; Voronina et al., 2011). Surveys performed in invertebrate model systems distinct from ecdysozoan phyla have been less explored, but begin to show promise in contributing to the body of scientific knowledge that drives advancements in reproductive medicine, as well as tempering of pests and parasites.

The phylum Platyhelminthes consists of free-living (planarians) and parasitic flatworms (trematodes, cestodes, and monogeneans). Planarians have long been studied for their ability to undergo whole-body regeneration and have emerged as model system in stem cell biology research (Elliott and Sanchez Alvarado, 2013; Newmark and Sanchez Alvarado, 2002; Rink, 2013; Shibata et al., 2010). These organisms can reproduce asexually by transverse fission, as well as sexually by hermaphroditic cross-fertilization (Newmark and Sanchez Alvarado, 2002; Newmark et al., 2008). Like mammals, planarians specify their germline through inductive mechanisms, whereas nematodes and flies utilize localized determinants (Extavour and Akam, 2003; Newmark et al., 2008; Wang et al., 2007). In fact, development of the planarian reproductive system occurs post-embryonically through differentiation of pluripotent stem cells, and can reoccur through a regenerative process upon injury (Chong et al., 2013; Collins et al., 2010; Newmark et al., 2008; Wang et al., 2007). An evolutionary novelty in the reproductive system of most flatworms is the presence of yolk glands (or vitellaria), which provide cellular material required for encapsulation and nutrition of embryos in ectolecithal eggs (Egger et al., 2015). This unique feature of flatworm reproduction makes yolk gland development a targetable mechanism for attenuating the dissemination and pathology of parasitic flatworms. Furthermore, sequence analyses have confirmed conservation of a fraction of human genes in planarians that are absent in genomes of ecdysozoan model systems (Sanchez Alvarado et al., 2002), and genetic contributions to development of the reproductive system can be studied by RNA interference (RNAi) (Wang et al., 2007). In sum, planarians are a valuable model for identifying genes involved in sexual reproduction of Platyhelminthes, as well as processes conserved across metazoan development.

Expression of Cytoplasmic Polyadenylation Element Binding protein (CPEB) homologs has been detected recently in the germline of the fluke *Schistosoma mansoni* and the non-parasitic flatworm *Macrostomum lignano* (Arbore et al., 2015; Cogswell et al., 2012; Lu et

al., 2016). Members of the CPEB family of proteins are key regulators of mRNA during metazoan germline development. CPEB proteins can be divided in two subfamilies: CPEB1 (classic CPEBs) and CPEB2. CPEB1 orthologs regulate maternal mRNAs during oogenesis and early development (Castagnetti and Ephrussi, 2003; Christerson and McKearin, 1994; Hake and Richter, 1994; Lantz et al., 1994; Stebbins-Boaz et al., 1996; Tan et al., 2001). CPEB2 homologs are expressed in mouse testes (Kurihara et al., 2003) and required for spermatogenesis in nematodes (Luitjens et al., 2000) and flies (Xu et al., 2012). Representatives of both CPEB1 and CPEB2 subfamilies are expressed in the brain, where they regulate mRNAs involved in courtship, pain, and long-term memory formation (Chao et al., 2013; Huang et al., 2006; Keleman et al., 2007; Pai et al., 2013; Rouhana et al., 2005; Si et al., 2003; Wu et al., 1998; Zearfoss et al., 2008). The binding specificity, target repertoire, and mechanisms of regulation by CPEB1 orthologs have been analyzed in several model systems (Darnell and Richter, 2012; Fernandez-Miranda and Mendez, 2012; Groisman et al., 2001; Richter, 2007). Classical CPEBs mediate translational repression and activation by modulating changes in poly(A) tail length. Cytoplasmic Polyadenylation Elements (CPEs; UUUUA(U/A)) present in the 3' untranslated regions (UTRs) recruit CPEB1 to target mRNAs (Barnard et al., 2004; Fox et al., 1989; Hake et al., 1998; Hake and Richter, 1994; Kim and Richter, 2006; Minshall et al., 1999, 2007; Novoa et al., 2010; Rouhana et al., 2005; Sheets et al., 1994). The binding specificity of CPEB2 subfamily members remains elusive. It has been reported that CPEB2 homologs bind to the same U-rich regulatory elements as CPEB1 (Afroz et al., 2014; Igea and Mendez, 2010; Novoa et al., 2010), but also to secondary RNA structures (Huang et al., 2006). Regulation of mRNA by CPEB2 has been shown to occur by poly(A) tail elongation (Igea and Mendez, 2010; Novoa et al., 2010; Ortiz-Zapater et al., 2012; Pique et al., 2008), poly(A) tail shortening (Hosoda et al., 2011), inhibition of translation independent of changes in poly(A) tail length (Huang et al., 2006), and nuclear functions (Kan et al., 2010).

In this study, we sought to uncover genetic mechanisms that regulate sexual reproduction of Platyhelminthes, utilizing the planarian *Schmidtea mediterranea* as a model system. We identified genes required for planarian oogenesis, spermatogenesis, and capsule formation, through the study of two *S. mediterranea* CPEB paralogs. We found that *Smed-CPEB1* is expressed exclusively in female organs, and is required for oogenesis and yolk gland development. *Smed-CPEB2* is expressed in testes and the central nervous system, and it is required for spermatogenesis as well as non-autonomously for development of ovaries and accessory reproductive organs. Transcriptome analyses of *Smed-CPEB1* and *Smed-CPEB2* knockdowns uncovered more than a hundred genes preferentially expressed in tissues of the reproductive system, a subset of which were functionally characterized by RNAi. Biochemical analyses support a model in which neuronal CPEB2 regulates expression of a signaling peptide required for sexual maturation. Collectively, these findings reveal molecular processes involved in metazoan germline development, as well as events specific to sexual reproduction of Platyhelminthes.

2. Results

2.1. Characterization of CPEB homologs in *Schmidtea mediterranea*

Two CPEB homologs (*Smed-CPEB1* and *Smed-CPEB2*) were identified in the *Schmidtea mediterranea* Genome Database (Robb et al., 2008, 2015) by performing TBLASTN searches against human CPEB1-4 protein sequences (Fig. 1A,A', and Supplementary Fig. 1A). Partial cDNAs were cloned based on genomic sequence and expression of mRNAs with corresponding sequence was verified by northern blot analysis (Supplementary Fig. 1B). Analysis of full-length ORF sequences obtained through 5' and 3' Rapid Amplification of cDNA Ends (RACE), revealed that both planarian CPEB homologs contain two RNA-recognition motifs (RRMs) and a Zinc Finger (ZnF) in their C-terminal ends, which is characteristic of CPEB protein architecture (Fig. 1B,C, and Supplementary Fig. 2A). *Smed-CPEB1* (GenBank: KU990884; Steiner et al., 2016) shares highest sequence conservation with members of the classical CPEB subfamily of proteins with known roles in oogenesis (Fig. 1A). Whole-mount *in situ* hybridization analysis (WMISH) revealed *Smed-CPEB1* expression exclusively in ovaries and yolk glands of sexually mature planarian hermaphrodites (Fig. 1D,D'). More specifically, ovarian *Smed-CPEB1* expression was detected in oocytes (Steiner et al., 2016), which are identifiable by their large size and condensed chromosomes (Fig. 1E). *Smed-CPEB2* (GenBank: KX074204) belongs to the CPEB2 protein subfamily (Fig. 1A). The C-terminal domain of this protein is 89% identical to the corresponding region of human CPEB2, which includes two RRMs and a ZnF (Fig. 1A' and Supplementary Fig. 2B). CPEB2 expression was detected in the planarian brain and testes by WMISH (Fig. 1F,F'). Detailed expression analysis by fluorescent *in situ* hybridization (FISH) revealed that CPEB2 transcripts accumulate in spermatogonia, peak in spermatocytes, and vanish in the later stages of spermatogenesis (Fig. 1G).

Given the germline expression of planarian CPEBs, as well as known functions of characterized CPEBs in other organisms, we hypothesized that *Smed-CPEB1* and *Smed-CPEB2* would be required for oogenesis and spermatogenesis, respectively. To test this hypothesis, we subjected groups of six sexually mature planarians (~1.5 cm long and actively laying capsules) to weekly feedings of double-stranded RNA (dsRNA). A control group, subjected to dsRNA corresponding to bacterial *ccdB* sequence, produced egg capsules throughout the 8-week experiment (Supplementary Fig. 3). Planarians subjected to *Smed-CPEB1* RNAi (*CPEB1(RNAi)*) or *Smed-CPEB2* RNAi (*CPEB2(RNAi)*) produced capsules at rates comparable to the control group during the first two weeks of the RNAi treatment, produced less capsules than controls during the third and fourth weeks of RNAi treatment, and ceased producing capsules altogether during the last four weeks (Supplementary Fig. 3). At the end of the 8-week RNAi treatment, testes development was evaluated by labeling with the nuclear stain 4', 6-Diamidino-2-Phenylindole, Dihydrochloride (DAPI), which facilitates visualization of organs with high cell density (*e.g.* copulatory apparatus, brain, pharynx), as well as sperm (Fig. 2A-D, A'-D'). The general anatomy of *CPEB1(RNAi)* appeared indistinguishable from that of control animals from this analysis (Fig. 2A,B). However, *CPEB2(RNAi)* displayed underdeveloped testes and copulatory apparatus (Fig. 2C). Similar, but more severe, defects were observed in *nanos(RNAi)* animals, which exhibit complete loss of germ cells (Fig. 2D; Wang et al.,

2007, 2010). Closer analysis of testis anatomy by confocal microscopy of control and *CPEB1(RNAi)* revealed normal production of spermatozoa (Fig. 2A',B'), which ultimately accumulated in the seminal vesicles (Fig. 2A,B). On the other hand, there were no spermatozoa or spermatids present in the under-developed testes of *CPEB2(RNAi)* (Fig. 2C'), suggesting that *Smed-CPEB2* is required for meiotic entry or early progression. The defect in spermatogenesis observed in *CPEB2(RNAi)* is less severe than the complete loss of testes observed after *nanos* RNAi (Fig. 2D'; Wang et al., 2007). From these results we conclude that *CPEB2* function is required for spermatogenesis and development of copulatory organs in *S. mediterranea*.

The presence of ovaries in *CPEB1(RNAi)* and *CPEB2(RNAi)* planarians was assessed by WMISH analysis of a *pumilio* homolog preferentially expressed in ovaries of *S. mediterranea* (Fig. 2E; Zayas et al., 2005). Ovaries were readily detected in control and *CPEB1(RNAi)* samples (Fig. 2E,F). However, ovaries were not detected in *CPEB2(RNAi)* planarians (Fig. 2G). To verify these observations, ovary development was analyzed in detail by confocal microscopy of samples subjected to DAPI staining and FISH analysis of *germinal histone H4* expression, which serves as a marker for oogonia (Wang et al., 2007; Rouhana et al., 2012). Indeed, ovaries were distinguishable in control and *CPEB1(RNAi)* planarians (Fig. 2H,I). Fully developed oocytes of approximately 20 µm in diameter and with condensed chromosomes were observed in control ovaries (Fig. 2H). However, *CPEB1(RNAi)* ovaries lacked oocytes and were filled with much smaller oogonia (Fig. 2I). Ovaries were not distinguishable in *CPEB2(RNAi)* samples, although presumptive oogonia were detected in the anatomical region of the ovaries (Fig. 2J). These results demonstrate that *Smed-CPEB1* is required for oogenesis in *S. mediterranea*, whereas *Smed-CPEB2* is required for development of the actual ovary. Altogether these results show that *S. mediterranea* CPEB homologs are required for germ cell development in gonads in which they are expressed. Additionally, *Smed-CPEB1* is required for yolk gland development (Steiner et al., 2016), whereas *Smed-CPEB2* is required for development of ovaries and accessory reproductive organs (e.g. copulatory apparatus) through non-autonomous mechanisms.

2.2. Characterization of the planarian reproductive system through analysis of *CPEB1(RNAi)* and *CPEB2(RNAi)* transcriptomes

The anatomical defects of *CPEB1(RNAi)* and *CPEB2(RNAi)* provided an opportunity to identify genes involved in sexual reproduction, particularly those expressed during later stages of oogenesis and spermatogenesis, as well as in accessory reproductive structures. Genes preferentially expressed in cell types absent in *CPEB1(RNAi)* (e.g. oocytes, yolk gland cells) and *CPEB2(RNAi)* (e.g. spermatids, spermatozoa, cells of the ovary and accessory reproductive organs) can be identified by comparing transcriptomes of control and CPEB knockdown planarians. Thus, we extracted total RNA from fertile control planarians and compared it with that of *CPEB1(RNAi)* and *CPEB2(RNAi)* animals of comparable size (Fig. 3A). Illumina reads from control (n=3 groups of 5 planarians; avg. reads/sample=20,605,364), *CPEB1(RNAi)* (avg. reads/sample=20,220,885), and *CPEB2(RNAi)* (avg. reads/sample=17,817,956) were mapped to a reference transcriptome composed of 55,949 contigs from *S. mediterranea* hermaphrodites (Rouhana et al., 2012). Comparison

between control and *CPEB1(RNAi)* samples revealed 618 genes with statistically significant differences in expression (> 2 -fold; $p < 0.05$; excluding contigs with ≥ 2 avg. mapped reads). Of these, 333 were under-represented and 285 significantly over-represented in RNA from *CPEB1(RNAi)* (Fig. 3B, Supplementary Table 1). Genes with largest fold-change reduction in *CPEB1(RNAi)* included homologs of ras family proteins, tetraspan 1, tial1 and calponin, while over-represented genes were led by core 1 glycoprotein-n-acetylgalactosamine 3-beta, actin and ran (small nuclear GTP)-binding protein (Supplementary Table 1). Enrichment of nucleic acid binding, RNA binding (but not DNA binding), ion channel activity, and receptor activity GO category functions were observed among genes under-represented in *CPEB1(RNAi)* (Supplementary Fig. 4). GO categories for biological processes including transport, transmembrane transport, ion transport, calcium ion transport and intracellular signaling were enriched among *CPEB1(RNAi)* under-represented sequences (Supplementary Fig. 4). Over-represented transcripts in *CPEB1(RNAi)* were enriched in GO categories such as nucleotide binding, nucleic acid binding, DNA binding, RNA binding, GTP binding, and transcription factor activity; whereas enriched biological process GO categories included regulation of transcription, protein transport and response to stress (Supplementary Fig. 4). It is possible that transcripts with altered expression in *CPEB1(RNAi)* represent mRNA targets whose stability depends on deadenylation or polyadenylation events mediated by Smed-CPEB1. However, it is likely that under-represented transcripts correspond to genes expressed in cell types missing after CPEB1 knockdown. On the other hand, over-represented transcripts may represent a signaling response (or loss of negative feedback) due to the absence of the missing cell types after *Smed-CPEB1* RNAi.

RNAseq analysis also revealed 1256 significantly under-represented and 808 over-represented transcripts from *CPEB2(RNAi)* samples (Fig. 3C, Supplementary Table 2). The genes with the largest increase in expression in *CPEB2(RNAi)* included Thrombospondin type 1 domain-containing protein, Aldolase, Porcupine-like protein and Cubitus interruptus homologs (Supplementary Table 2). Tetraspan 1, Surfactant b, and a conserved Plasmodium protein also identified in *CPEB1(RNAi)*, were among the genes with the largest reduction in *CPEB2(RNAi)* (Supplementary Table 2). Enriched GO functional categories among under-represented sequences in *CPEB2(RNAi)* included hydrolase activity and peptidase activity, whereas the categories of DNA binding, nucleic acid binding and RNA binding were enriched among over-represented sequences (Supplementary Fig. 5). Biological processes enriched in *CPEB2(RNAi)* under-represented sequences include proteolysis and microtubule-based movement, whereas over-represented sequences included DNA integration, regulation of transcription, RNA-dependent DNA replication and G-protein coupled receptor signaling (Supplementary Fig. 5). Given the absence of ovaries, functional testes, and accessory reproductive organs in *CPEB2(RNAi)*, we expect that many of the 1256 underrepresented sequences correspond to genes normally expressed in these structures. As with *Smed-CPEB1*, it is also possible that transcripts with altered expression in these samples represent *Smed-CPEB2* target mRNAs, particularly in neurons, where Smed-CPEB2 expression was evident (Fig. 1F).

To establish markers for studying the anatomy of the planarian reproductive system, we performed WMISH analysis for transcripts with reduced abundance in *CPEB1(RNAi)*

and/or *CPEB2(RNAi)*. We first focused on fifty-two genes identified in *Smed-CPEB1(RNAi)* transcriptomes (Supplementary Table 3), which were prioritized based on largest fold-change of expression, detection of conserved domains through homology searches, and availability of cDNA clones prepared in our laboratory (Zayas et al., 2005). Expression in ovaries was verified by WMISH for 26 of these genes, which included a *gelsolin* homolog that labels ovarian cells facing the tuba (Fig. 3D). Four of the thirteen genes with the largest decrease in transcript abundance after *CPEB1 RNAi* displayed expression patterns reflective of yolk gland distribution (Supplementary Table 3). These included two previously characterized genes, *surfactant b* and *synaptotagmin XV* (Steiner et al., 2016), an uncharacterized protein conserved in the choanoflagellate *Monosiga brevicollis* (Fig. 3E), and a gene homologous to a protein identified in *Plasmodium* (Contig5529; PL030017B20H10; Supplementary Fig. 6). Reduction of all these yolk gland markers validates the previously reported requirement of *Smed-CPEB1* function for yolk gland development (Steiner et al., 2016) and explains the loss of capsule production observed after *CPEB1 RNAi* (Supplementary Fig. 3).

Investigation of candidates identified from *CPEB2(RNAi)* transcriptome analysis included 132 sequences. Enriched expression in the testes was detected for 56 of these sequences (Fig. 3F, Supplementary Table 4). Markers were also identified for accessory reproductive organs such as the penis papilla (*Cre-*alp1* protein*, Fig. 3G), the oviducts (a homolog of a hypothetical protein conserved in *Schistosoma mansoni*; PL04015A2A04; Fig. 3H), glands surrounding the gonopore (*tetraspanin 66e*; Fig. 3I), and yolk glands (see below). The high representation of testes markers (43.1%) is likely due to the abundance of this tissue in the planarian (Fig. 1F, 2A). Altogether, the transcriptomic analyses of *CPEB1(RNAi)* and *CPEB2(RNAi)* identified over a hundred genes specifically expressed in structures of the planarian reproductive system.

2.3. Identification of yolk gland genes required for capsule tanning

The capsules that house planarian embryos are produced independently from ovulation, fertilization or mating (Steiner et al., 2016). The capsule shell is initially formed in the genital atrium, which is located inside the gonopore posterior to the pharynx (Fig. 4A). These capsules are filled by hundreds of yolk cells that nurture the developing embryo (Martin-Duran et al., 2008; Shinn, 1993). Upon deposition, capsules undergo a “quinone tanning” process in which the proteinaceous shell hardens and darkens from yellow to dark-brown hues (Fig. 4B). Although materials required for capsule shell formation and tanning are believed to be contributed by yolk cells, little is known about the genetic factors contributing to this process.

Genes expressed in patterns reflective of yolk gland distribution were identified in both *CPEB1(RNAi)* and *CPEB2(RNAi)* transcriptomes (Fig. 4C-G; Supplementary Tables 3 and 4). From these, four were found to be required for capsule shell pigmentation (Fig. 4H-L). One encodes an uncharacterized protein, which we named *Smed-tanning factor-1 (tan-1)* (Fig. 4D). The other three genes encode homologs of Surfactant B, Tyrosinase, and C-type lectin (Fig. 4E-G). Expression of *tyrosinase* was also strongly detected posterior to the copulatory complex (Fig. 4F). Capsules produced by *tan-1(RNAi)* animals developed a dark

reddish hue comparable to that of normal capsules 4–8 h post-deposition (Fig. 4B, I), but failed to reach the dark brown color observed in normal capsules (Fig. 4H). Capsules from *surfactant b(RNAi)* and *tyrosinase(RNAi)* developed more severe coloration defects, maintaining yellow to orange hues comparable to those of normal capsules 30 min to 2 h post-deposition (Fig. 4J, K). *c-type lectin(RNAi)* capsules displayed the most severe shell coloration defect, manifested with an overall milky color and a few dark speckles (Fig. 4L). The capsule coloration defects observed for all four genes lasted for at least three months. Additionally, no hatchlings emerged from any of the capsules that displayed coloration defects during this time (*tan-1*, n=12; *surfactant b*, n=18; *tyrosinase*, n=8; and *c-type lectin*, n=12), suggesting that “tanning” and/or processes that lead to capsule maturation are essential for planarian embryonic development. These processes may also play a role in reproduction of parasitic flatworms, since a subset of these genes is conserved in schistosomes and/or tapeworms (Supplementary Table 5).

2.4. A Synaptotagmin homolog required for capsule shell assembly

Another gene with reduced transcript levels in both *CPEB1(RNAi)* and *CPEB2(RNAi)* encodes a synaptotagmin-like family member (*Smed-synaptotagmin XV* or *sytXV*). Detection of *sytXV* expression by WISH (Fig. 5A) is confined to the ovaries (Fig. 5A') and yolk glands (Fig. 5A''). More specifically, ovarian *sytXV* expression has been shown in oocytes (Steiner et al., 2016). Using *Smed-CPEB1* as a marker for oogenesis and yolk gland development, analyses by WMISH showed that neither process is affected in *sytXV(RNAi)* (Fig. 5B,C). However, analysis of capsule production by *sytXV(RNAi)* animals revealed that they produce defective structures during deposition (Fig. 5D,E). The aberrant capsules produced by *sytXV(RNAi)* contained a thin membrane holding the yolk cells together, but this fragile structure eventually collapsed without yielding hatchlings. These results suggest that *sytXV* function has a direct role in capsule assembly, and possibly mediates exocytic release of yolk cell material required for shell formation.

2.5. A germline eIF4E paralog is required for oogenesis in *S. mediterranea*

Functional analysis of a eukaryotic translation initiation factor 4E homolog (*Smed-eIF4E-like*) underrepresented in *CPEB1(RNAi)* transcriptomes revealed a pleiotropic phenotype. *Smed-eIF4E-like* expression was detected in ovaries, testes, and a subset of gut cells, presumably goblet cells (Fig. 5F-F''). Analysis of comparably sized samples revealed that *eIF4E-like(RNAi)* ovaries contained reduced oocyte numbers compared to controls (1.5 oocytes/ovary vs. 4.7 oocytes/ovary, $p < 0.05$ two-tailed unpaired Student's *t*-test) (Fig. 5G,H). On the other hand, the number of non-oogenic cells in the ovary, visualized by *gelsolin* FISH, was higher in *eIF4E-like(RNAi)* than in control ovaries (Fig. 5G,H; 77.0 *gelsolin* (+) cells/ovary vs. 25.7 *gelsolin* (+) cells/ovary, $p < 0.05$ two-tailed unpaired Student's *t*-test). Spermatogenesis defects were not observed in *eIF4E-like(RNAi)* animals compared with control samples of the same size (data not shown). However, a significant reduction in capsule production (Supplementary Fig. 7), along with a growth defect (avg. size post-fixation=0.81 cm vs. 0.51 cm, $p < 0.01$ two-tailed unpaired Student's *t*-test) were observed in *eIF4E(RNAi)* after prolonged (4 weeks) RNAi treatments. We conclude that the function of this eIF4E paralog is required for oocyte development and hypothesize that

the reduction in capsule production may result from growth defects observed after prolonged *Smed-eIF4E-like* RNAi.

2.6. Identification of conserved factors required in late stages of planarian spermatogenesis

Given the defects in spermatogenesis observed in *CPEB2(RNAi)* testes (Fig. 2C), we hypothesized that genes under-represented in *Smed-CPEB2(RNAi)* transcriptomes include factors required for sperm elongation and function. We tested 57 candidate genes with validated testis expression (Supplementary Table 4) for spermatogenesis defects after RNAi. Defects in maintenance of sperm production by sexually mature planarians were visualized by DAPI staining and confocal microscopy at the end of a 6-week RNAi treatment. Six genes were found to be required for proper sperm development (Fig. 6A-F). From these genes, *Smed-rap55* (RNA-associated protein 55 (RAP55/LSM14)) was previously reported to function in planarian spermatid elongation (Wang et al., 2010), thus validating our approach. The five other genes found to be required for spermatid elongation are planarian homologs of *cysteine/histidine rich-1* (*Smed-cyhr-1*), the SWI/SNF chromatin remodeling complex component *SMARCB1*, *polyubiquitin2*, as well as *t-complex protein alpha* (*Smed-cct-1*) and *t-complex protein delta* (*Smed-cct-4*) (Fig. 6B-F). Together with the identification of factors required for capsule development and oogenesis, this study provides a set of candidate genes with functions specific to sexual reproduction of flatworms (yolk gland genes), as well as genes with conserved roles in metazoan germline development.

2.7. CPEB2(RNAi) leads to decreased Neuropeptide Y-8 levels

The fact that *Smed-CPEB2* RNAi affected the development of tissues in which its expression was not detected (e.g., ovaries, copulatory apparatus and yolk glands), led us to hypothesize that regulation of neuronal mRNAs by CPEB2 is required for development of these structures. A natural target for CPEB2 under this model is *neuropeptide Y-8* (*npy-8*), which is required for sexual maturation; knockdown of this gene closely phenocopies *CPEB2(RNAi)* (Collins et al., 2010). Analysis of the *npy-8* mRNA 3'-UTR revealed the presence of sequence sufficient for human CPEB2 binding in vitro (UUUUA; Afroz et al., 2014) (Fig. 7A), suggesting the possibility for direct *Smed-CPEB2* binding. Furthermore, co-expression analysis by FISH demonstrated that neurons expressing *npy-8* also contain *Smed-CPEB2* transcripts (Fig. 7B-B''). We tested whether *npy-8* expression levels were affected by *CPEB2* RNAi by northern blot as well as RT-qPCR, and found *npy-8* mRNA was ~45% less abundant in total RNA extracts of *CPEB2(RNAi)* compared to control(*RNAi*) or *CPEB1(RNAi)* samples (Fig. 7C,D). Analysis by western blot using anti-NPY-8 antibodies (Saber et al., in revision) revealed that the NPY-8 peptide present in extracts of control and *CPEB1(RNAi)* planarians was dramatically reduced in *CPEB2(RNAi)* extracts (Fig. 7E). Thus, inhibition of *Smed-CPEB2* expression leads to a severe reduction in NPY-8 peptide levels. These results support the model that *Smed-CPEB2* regulates sexual maturation non-autonomously through stimulation of *npy-8* mRNA translation in neurons.

3. Discussion

To examine the contributions of cytoplasmic polyadenylation to germ cell biology, we characterized the expression and function of CPEB homologs in *S. mediterranea*. We showed that *Smed-CPEB1* is expressed in the ovaries and yolk glands of sexually mature planarians, while *Smed-CPEB2* is expressed in the testes and central nervous system. *Smed-CPEB1* is required for planarian oogenesis and yolk gland development, whereas *Smed-CPEB2* is required for spermatogenesis as well as for sexual maturation through a non-autonomous mechanism involving regulation of *neuropeptide y-8* expression. This study complements previous work (Chong et al., 2011; Wang et al., 2010) in providing a collection of markers for the study of the planarian reproductive system. We identified markers for different components of the planarian reproductive system, including but not limited to the testes, distinct ovarian cell types, the oviducts, the penis papilla, and yolk glands.

Functional analysis of candidates with validated expression in ovaries, testes, and yolk glands, led to the identification of 11 genes required for germline development and/or sexual reproduction in *S. mediterranea*. These include genes encoding proteins with uncharacterized domains (*i.e. tanning factor-1*), and genes with characterized homologs not previously known to play a role in germline development (*e.g. SMARCB1* and *cyhr1*). We identified two planarian genes required for spermatid elongation (*cct-1* and *cct-4*) that encode components of the chaperonin containing TCP-1 (CCT) complex. The CCT complex is highly conserved in eukaryotes and key for actin and tubulin folding (Valpuesta et al., 2002). *SMARCB1* belongs to the family of switch/sucrose nonfermentable (SWI/SNF) chromatin remodeling complex proteins, and is the second component of this complex shown to be required for planarian spermatogenesis. Wang et al. (Wang et al., 2010) previously showed that the central catalytic ATPase of the SWI/SNF complex, the *brahma-related gene 1* homolog (*Smed-Brg1*; or *SMARCA4*) is required for spermatid elongation. Mammalian orthologs of these genes have broad expression patterns, but their analysis in *S. mediterranea* revealed functional requirements during spermatogenesis, which demonstrates one advantage of using different model systems for studying germline development. Recent evidence shows that the contributions of SWI/SNF factors uncovered in planarian spermatogenesis studies hold true in mammals, as knockout of *Brg1* in mouse testes leads to arrest of sperm development at midpachytene stage (Kim et al., 2012; Wang et al., 2012). Similarly, current tools for tissue-specific knockout studies in mice can facilitate analysis of mammalian orthologs of other genes characterized in planarians, and determine the conservation of molecular pathways contributing to metazoan germline development.

Twenty-six genes with ovarian expression were identified through RNAseq analysis of *CPEB1(RNAi)*. Amongst these, an eIF4E homolog was found to be required for oogenesis (Fig. 5H). This result corroborates reports from the study of a homolog in nematodes (*ife-1*; Henderson et al., 2009). Interestingly, an ovary-specific isoform of eIF4E (eIF4Eb) was identified as a component of CPEB-containing complexes in *Xenopus* oocytes (Minshall et al., 2007). Contrary to canonical eIF4E, which binds the 5'-cap and facilitates recruitment of ribosomes, eIF4Eb appears to inhibit translation of mRNAs (Kubacka et al., 2015; Minshall et al., 2007). Indeed, our experiments show that both *CPEB1* and *eiF4e-like* are required for

development of oocytes in *S. mediterranea*, so these may function as a complex in this context.

Like *Smed-CPEB1*, expression of *sytXV* is restricted to yolk glands and ovaries (Fig. 5A), more specifically oocytes (Steiner et al., 2016). However, *sytXV* RNAi did not lead to defects in oogenesis or yolk gland development (Fig. 5C), instead it resulted in a severe capsule shell formation defect (Fig. 5E). This defect is attributed to disruption of *sytXV* expression in yolk cells, since it has been shown that oocytes are dispensable for normal capsule formation (Steiner et al., 2016). Synaptotagmin proteins play a role in regulating exocytosis that has been primarily studied in neurons (Sudhof, 2002). This family of proteins is characterized by the presence of an N-terminal transmembrane region and two C₂ domains. *Smed-SytXV* is more similar to Syt14 and Syt15 than any other mouse protein, it contains two C₂ domains but does not have a transmembrane region recognizable by domain prediction software (i.e. TMpred, TMHMM). Thus the particular phenotype of *Smed-sytXV(RNAi)* could be explained by a reduction of *SytXV*-mediated secretion of yolk factors required for shell matrix formation. Indeed, yolk cells contain granules with materials that are released by exocytosis and form the capsule shell (or “wall”; Shinn, 1993), and the identification of *sytXV* function in this process paves the way for dissecting the molecular events involved in capsule shell formation.

Four additional genes required for development of the capsule shell were identified (Fig. 4). Yolk cells inside the developing capsule are thought to secrete proteins rich in 3,4-dihydroxyphenyl-L-alanine (DOPA) and enzymes that oxidize DOPA into α -quinone, which ultimately polymerizes with other proteins to harden and pigment the shell (Gremigni and Domenici, 1974; Ishida and Teshirogi, 1986; Marinelli, 1972; Nurse, 1950). Indeed, all four genes found to contribute to the tanning process are expressed in yolk glands, providing additional evidence for the contribution of yolk cells to shell development. Among these, Tyrosinase is known to catalyze polymerization of proteins *in vitro* and to be involved in the quinone tanning process through DOPA modifications of tyrosine-rich proteins in Platyhelminthes and insects (Ishida and Teshirogi, 1986; Waite, 1983). It is not clear how other yolk cell gene products influence the quinone tanning process, but it seems clear that the molecular events associated with this process are required for planarian embryonic development, since capsules with pigmentation defects failed to yield any hatchlings. Identification of proteins required for capsule shell formation may prove valuable in medical efforts to attenuate egg (capsule) production by parasitic flatworms.

CPEB homologs are key factors for post-transcriptional regulation during germline development and in neurons. The RNA-binding domain of human CPEB2 subfamily members shares 85% amino acid sequence identity with *Smed-CPEB2* (Fig. 1A', Supplementary Fig. 2), suggesting that mechanisms for target recognition and regulation are likely conserved between planarians and mammals. Although modulation of neuropeptide expression is not a known function of mammalian CPEB homologs, regulation of a conserved handful of brain mRNAs by cytoplasmic polyadenylation has been reported in flies, *Aplysia*, *Xenopus*, and mice (Gerstner et al., 2012; Ivshina et al., 2014; Rouhana et al., 2005). Future research will uncover the identity and fate of mRNAs regulated by *Smed-CPEB2* in neurons and testes, which will reveal additional pathways involved in sexual

maturation cell autonomously (regulation of proliferation and differentiation in sperm precursors) and non-autonomously (by modulation of neuronal signaling).

4. Materials and methods

4.1. Planarian culture

Laboratory lines of hermaphroditic *Schmidtea mediterranea* (Zayas et al., 2005) were used for all experiments and maintained in 0.75X Montjuïc salts as per (Wang et al., 2007). Animals were fed calf liver and starved for a week prior to experimentation. Capsules were collected weekly, maintained and monitored in 0.75X Montjuïc salts at 18 °C for 2 months post-deposition.

4.2. Whole-mount in situ hybridization and DAPI staining

Sample fixation for WMISH and DAPI staining was performed as per (King and Newmark, 2013) with modifications for large planarians that include 7–10 min treatment with 10% N-acetyl cysteine in PBS, and a 1.5 h fixation at 4 °C using 4% formaldehyde in PBSTx (PBS; 0.3% Triton-X). Hybridization of riboprobes was extended to 36 h. Colorimetric signal development was performed as per (Pearson et al., 2009). Nuclei were stained by incubation in PBSTx solution containing 5 µg/mL 4',6-diamidino-2-phenylindole (DAPI) overnight at 4 °C, followed by four washes in PBSTx. Low-magnification images were captured with Zeiss V.12 and V.16 SteREO units, and high-magnification images by confocal microscopy.

4.3. RNA-interference

RNAi was performed as per (Rouhana et al., 2013). Briefly, groups of six to seven planarians were fed to satiation with liver solution containing dsRNA (100 ng/µL concentration) every 5–7 days. DsRNA of bacterial *ccdB* gene sequence was used as a negative control.

4.4. RNAseq analysis

Total RNA from biological triplicates of control(RNAi), *CPEB1(RNAi)* and *CPEB2(RNAi)* planarians (> 1.5 cm) was extracted using TRIzol (Invitrogen), treated with RQ1 DNase (Promega) for 10 min at room temperature, extracted again with TRIzol, dissolved in RNase-free water, and submitted to the Roy J. Carver Biotechnology Center (Univ. of Illinois at Urbana-Champaign) for library preparation (Illumina TruSeq RNA Sample prep kit) and sequencing (Illumina HiSeq. 2000 version 5 chemistry and analysis pipeline 1.8). Sequence reads were mapped to a *S. mediterranea* hermaphrodite reference transcriptome (Rouhana et al., 2012; “uc_Smed_v2” in PlanMine (Brandl et al., 2016)) and quantified using CLC genomics workbench (Qiagen) under default settings as in (Rouhana et al., 2012). The sequence dataset generated from RNAseq is publicly available (BioProject ID PRJNA319057).

4.5. Northern blot and RT-qPCR

Riboprobes corresponding to partial *Smed-CPEB1* and *Smed-CPEB2* ORFs, including RRM and ZnF domains, were synthesized using T3 polymerase from pJC53.2/*Smed-*

CPEB1 and pJC53.2/*Smed-CPEB2*, and used in northern blots as per (Miller and Newmark, 2012). Methods used for quantification of *npy-8* mRNA by northern blot and RT-qPCR have been described (Collins et al., 2010).

4.6. 5' and 3' Rapid Amplification of cDNA Ends (RACE)

Full-length cDNAs were obtained using a SMARTer[®] RACE 5'/3' Kit (Clontech Laboratories) as per manufacturer protocol. The primers used were: *Smed-CPEB1* 5' RACE, 5'-GATTACGCCAAGCTTCGTGTTGAGAATT AAATGTTTGTG-3'; *Smed-CPEB1* 3' RACE, 5'-GATTACGCCAAGCTTAACTCCAGCCTTAAAGACATTTG-3'; *Smed-CPEB2* 5' RACE, 5'-GATTACGCCAAGCTTATTGGTGAATTTATCGAATCATAG-3'; and *Smed-CPEB2* 3' RACE, 5'-GATTACGCCAAGCTTAGCTATTGAATTGGCAATGATTATG-3'.

4.7. NPY-8 Extraction and Western Blot

Planarian neuropeptides were extracted using a modification of published methods (Sturm et al., 2010) prior to detection by western blot. Endogenous proteases were inactivated by incubating worms at 80 °C for 1 min and samples were frozen on dry ice, transferred to a chilled glassteflon or glass-glass (small clearance) homogenizer and homogenized by 20 strokes in 1 mL acidified methanol (methanol, acetic acid, and water at 90:9:1;) for every 5 worms. The homogenate was stirred at 4 °C for an hour and centrifuged at > 14,000g for 20 min. The supernatant was frozen in liquid nitrogen, vacuum-dried overnight, and the pellet was solubilized in 100 µL of 1X lithium dodecyl sulfate (LDS) sample buffer containing 100 mM DTT by incubation at 70–80 °C for 10 min. 10 µL of the supernatant was loaded on a NuPAGE Novex 12% Bis-Tris gel (Invitrogen), resolved in 2-ethanesulfonic (MES) running buffer, and transferred onto a presoaked Immobilon-P[®] membrane in 2X NuPAGE Transfer Buffer (Invitrogen) containing 20% methanol at 10 V for 40 min. After transfer, the membrane was air-dried for 2 h and incubated in 5% BSA, 1% casein, and affinity-purified anti-NPY-8 antibody (1:2000 dilution) in PBS containing 0.05% Tween-20 (PBSTw) for 4 h at 4 °C. After three PBSTw washes, incubation with HRP-conjugated anti-rabbit antibodies (Jackson Laboratories; 1:10,000), and additional washes in PBSTw, the membrane was treated with ECL Western Blot Detection Reagent (Amersham) and imaged with a FluorChem Q system (Alpha Innotech).

Supplementary Material

Refer to Web version on PubMed Central for supplementary material.

Acknowledgments

We thank: Alvaro Hernandez and the Roy J. Carver Biotechnology Center for superb assistance with RNA-seq processing; the Agata laboratory for guidance and support during the initial analysis of planarian CPEB homologs; Jennifer Weiss, Maribel Arteaga and Steve Sayson for assisting with in situ hybridization and RNAi.

Funding

This work was supported, in part, by a Ford Foundation Postdoctoral Fellowship to LR and by the National Institutes of Health [R15 HD082754 to LR, R01 HD043403 to PAN]. JT is supported by a Japanese Society for the

Promotion of Science Overseas Research Fellowship. PAN is an investigator of the Howard Hughes Medical Institute.

References

- Afroz T, Skrisovska L, Belloc E, Guillen-Boixet J, Mendez R, Allain FH. A fly trap mechanism provides sequence-specific RNA recognition by CPEB proteins. *Genes Dev.* 2014; 28:1498–1514. [PubMed: 24990967]
- Arbore R, Sekii K, Beisel C, Ladurner P, Berezikov E, Schärer L. Positional RNA-Seq identifies candidate genes for phenotypic engineering of sexual traits. *Front Zool.* 2015; 12:14. [PubMed: 26146508]
- Barnard DC, Ryan K, Manley JL, Richter JD. Symplekin and xGLD-2 are required for CPEB-mediated cytoplasmic polyadenylation. *Cell.* 2004; 119:641–651. [PubMed: 15550246]
- Brandl H, Moon H, Vila-Farre M, Liu SY, Henry I, Rink JC. PlanMine—a mineable resource of planarian biology and biodiversity. *Nucleic Acids Res.* 2016; 44:D764–773. [PubMed: 26578570]
- Castagnetti S, Ephrussi A. Orb and a long poly(A) tail are required for efficient oskar translation at the posterior pole of the *Drosophila* oocyte. *Development.* 2003; 130:835–843. [PubMed: 12538512]
- Chao HW, Tsai LY, Lu YL, Lin PY, Huang WH, Chou HJ, Lu WH, Lin HC, Lee PT, Huang YS. Deletion of CPEB3 enhances hippocampus-dependent memory via increasing expressions of PSD95 and NMDA receptors. *J Neurosci.* 2013; 33:17008–17022. [PubMed: 24155305]
- Chong T, Collins JJ 3rd, Brubacher JL, Zarkower D, Newmark PA. A sex-specific transcription factor controls male identity in a simultaneous hermaphrodite. *Nat Commun.* 2013; 4:1814. [PubMed: 23652002]
- Chong T, Stary JM, Wang Y, Newmark PA. Molecular markers to characterize the hermaphroditic reproductive system of the planarian *Schmidtea mediterranea*. *BMC Dev Biol.* 2011; 11:69. [PubMed: 22074376]
- Christerson LB, McKearin DM. orb is required for anteroposterior and dorsoventral patterning during *Drosophila* oogenesis. *Genes Dev.* 1994; 8:614–628. [PubMed: 7926753]
- Cogswell AA, Kommer VP, Williams DL. Transcriptional analysis of a unique set of genes involved in *Schistosoma mansoni* female reproductive biology. *PLoS Negl Trop Dis.* 2012; 6:e1907. [PubMed: 23166854]
- Collins JJ 3rd, Hou X, Romanova EV, Lambrus BG, Miller CM, Saberi A, Sweedler JV, Newmark PA. Genome-wide analyses reveal a role for peptide hormones in planarian germline development. *PLoS Biol.* 2010; 8:e1000509. [PubMed: 20967238]
- Darnell JC, Richter JD. Cytoplasmic RNA-binding proteins and the control of complex brain function. *Cold Spring Harb Perspect Biol.* 2012; 4:a012344. [PubMed: 22723494]
- Egger B, Lapraz F, Tomiczek B, Müller S, Dessimoz C, Girstmair J, Skunca N, Rawlinson KA, Cameron CB, Beli E, et al. A transcriptomic-phylogenomic analysis of the evolutionary relationships of flatworms. *Curr Biol.* 2015; 25:1347–1353. [PubMed: 25866392]
- Elliott SA, Sanchez Alvarado A. The history and enduring contributions of planarians to the study of animal regeneration. *Wiley Interdiscip Rev Dev Biol.* 2013; 2:301–326. [PubMed: 23799578]
- Extavour CG, Akam M. Mechanisms of germ cell specification across the metazoans: epigenesis and preformation. *Development.* 2003; 130:5869–5884. [PubMed: 14597570]
- Fernandez-Miranda G, Mendez R. The CPEB-family of proteins, translational control in senescence and cancer. *Ageing Res Rev.* 2012; 11:460–472. [PubMed: 22542725]
- Fox CA, Sheets MD, Wickens MP. Poly(A) addition during maturation of frog oocytes: distinct nuclear and cytoplasmic activities and regulation by the sequence UUUUUAU. *Genes Dev.* 1989; 3:2151–2162. [PubMed: 2628165]
- Gerstner JR, Vanderheyden WM, LaVaute T, Westmark CJ, Rouhana L, Pack AI, Wickens M, Landry CF. Time of day regulates subcellular trafficking, tripartite synaptic localization, and polyadenylation of the astrocytic Fabp7 mRNA. *J Neurosci.* 2012; 32:1383–1394. [PubMed: 22279223]

- Gremigni V, Domenici L. Electron microscopical and cytochemical study of vitelline cells in the fresh water triclad *Dugesia lugubris* s. 1. I. Origin and morphogenesis of cocoon-shell globules. *Cell Tissue Res.* 1974; 150:261–270. [PubMed: 4367991]
- Groisman I, Huang YS, Mendez R, Cao Q, Richter JD. Translational control of embryonic cell division by CPEB and maskin. *Cold Spring Harb Symp Quant Biol.* 2001; 66:345–351. [PubMed: 12762037]
- Hake LE, Mendez R, Richter JD. Specificity of RNA binding by CPEB: requirement for RNA recognition motifs and a novel zinc finger. *Mol Cell Biol.* 1998; 18:685–693. [PubMed: 9447964]
- Hake LE, Richter JD. CPEB is a specificity factor that mediates cytoplasmic polyadenylation during *Xenopus* oocyte maturation. *Cell.* 1994; 79:617–627. [PubMed: 7954828]
- Henderson MA, Cronland E, Dunkelbarger S, Contreras V, Strome S, Keiper BD. A germline-specific isoform of eIF4E (IFE-1) is required for efficient translation of stored mRNAs and maturation of both oocytes and sperm. *J Cell Sci.* 2009; 122:1529–1539. [PubMed: 19383718]
- Hosoda N, Funakoshi Y, Hirasawa M, Yamagishi R, Asano Y, Miyagawa R, Ogami K, Tsujimoto M, Hoshino S. Anti-proliferative protein Tob negatively regulates CPEB3 target by recruiting Caf1 deadenylase. *EMBO J.* 2011; 30:1311–1323. [PubMed: 21336257]
- Huang YS, Kan MC, Lin CL, Richter JD. CPEB3 and CPEB4 in neurons: analysis of RNA-binding specificity and translational control of AMPA receptor *GluR2* mRNA. *EMBO J.* 2006; 25:4865–4876. [PubMed: 17024188]
- Igea A, Mendez R. Meiosis requires a translational positive loop where CPEB1 ensues its replacement by CPEB4. *EMBO J.* 2010; 29:2182–2193. [PubMed: 20531391]
- Ishida S, Teshirogi W. Eggshell Formation in Polyclads (Turbellaria). *Hydrobiologia.* 1986; 132:127–135.
- Ivshina M, Lasko P, Richter JD. Cytoplasmic polyadenylation element binding proteins in development, health, and disease. *Annu Rev Cell Dev Biol.* 2014; 30:393–415. [PubMed: 25068488]
- Kan MC, Oruganty-Das A, Cooper-Morgan A, Jin G, Swanger SA, Bassell GJ, Florman H, van Leyen K, Richter JD. CPEB4 is a cell survival protein retained in the nucleus upon ischemia or endoplasmic reticulum calcium depletion. *Mol Cell Biol.* 2010; 30:5658–5671. [PubMed: 20937770]
- Keleman K, Kruttner S, Alenius M, Dickson BJ. Function of the *Drosophila* CPEB protein Orb2 in long-term courtship memory. *Nat Neurosci.* 2007; 10:1587–1593. [PubMed: 17965711]
- Kim JH, Richter JD. Opposing polymerase-deadenylase activities regulate cytoplasmic polyadenylation. *Mol Cell.* 2006; 24:173–183. [PubMed: 17052452]
- Kim Y, Fedoriw AM, Magnuson T. An essential role for a mammalian SWI/ SNF chromatin-remodeling complex during male meiosis. *Development.* 2012; 139:1133–1140. [PubMed: 22318225]
- Kimble J. Molecular regulation of the mitosis/meiosis decision in multicellular organisms. *Cold Spring Harb Perspect Biol.* 2011; 3:a002683. [PubMed: 21646377]
- Kimmins S, Sassone-Corsi P. Chromatin remodelling and epigenetic features of germ cells. *Nature.* 2005; 434:583–589. [PubMed: 15800613]
- King RS, Newmark PA. In situ hybridization protocol for enhanced detection of gene expression in the planarian *Schmidtea mediterranea*. *BMC Dev Biol.* 2013; 13:8. [PubMed: 23497040]
- Kubacka D, Miguel RN, Minshall N, Darzynkiewicz E, Standart N, Zuberek J. Distinct features of cap binding by eIF4E1b proteins. *J Mol Biol.* 2015; 427:387–405. [PubMed: 25463438]
- Kurihara Y, Tokuriki M, Myojin R, Hori T, Kuroiwa A, Matsuda Y, Sakurai T, Kimura M, Hecht NB, Uesugi S. CPEB2, a novel putative translational regulator in mouse haploid germ cells. *Biol Reprod.* 2003; 69:261–268. [PubMed: 12672660]
- Lantz V, Chang JS, Horabin JI, Bopp D, Schedl P. The *Drosophila orb* RNA-binding protein is required for the formation of the egg chamber and establishment of polarity. *Genes Dev.* 1994; 8:598–613. [PubMed: 7523244]
- Lu Z, Sessler F, Holroyd N, Hahnel S, Quack T, Berriman M, Greveling CG. Schistosome sex matters: a deep view into gonad-specific and pairing-dependent transcriptomes reveals a complex gender interplay. *Sci Rep.* 2016; 6:31150. [PubMed: 27499125]

- Luitjens C, Gallegos M, Kraemer B, Kimble J, Wickens M. CPEB proteins control two key steps in spermatogenesis in *C. elegans*. *Genes Dev.* 2000; 14:2596–2609. [PubMed: 11040214]
- Marinelli M. Observations on the shell formation in the cocoon of *Dugesia lugubris* s.l. *Boll Zool.* 1972; 39:337–341.
- Martin-Duran JM, Duocastella M, Serra P, Romero R. New method to deliver exogenous material into developing planarian embryos. *J Exp Zool Part B: Mol Dev Evol.* 2008; 310:668–681.
- Miller CM, Newmark PA. An insulin-like peptide regulates size and adult stem cells in planarians. *Int J Dev Biol.* 2012; 56:75–82. [PubMed: 22252538]
- Minshall N, Reiter MH, Weil D, Standart N. CPEB interacts with an ovary-specific eIF4E and 4E-T in early *Xenopus* oocytes. *J Biol Chem.* 2007; 282:37389–37401. [PubMed: 17942399]
- Minshall N, Walker J, Dale M, Standart N. Dual roles of p82, the clam CPEB homolog, in cytoplasmic polyadenylation and translational masking. *RNA.* 1999; 5:27–38. [PubMed: 9917064]
- Newmark PA, Sanchez Alvarado A. Not your father's planarian: a classic model enters the era of functional genomics. *Nat Rev Genet.* 2002; 3:210–219. [PubMed: 11972158]
- Newmark PA, Wang Y, Chong T. Germ cell specification and regeneration in planarians. *Cold Spring Harb Symp Quant Biol.* 2008; 73:573–581. [PubMed: 19022767]
- Novoa I, Gallego J, Ferreira PG, Mendez R. Mitotic cell-cycle progression is regulated by CPEB1 and CPEB4-dependent translational control. *Nat Cell Biol.* 2010; 12:447–456. [PubMed: 20364142]
- Nurse FR. Quinone Tanning in the Cocoon-Shell of *Dendrocoelum lacteum*. *Nature.* 1950; 165:570–570.
- Ortiz-Zapater E, Pineda D, Martinez-Bosch N, Fernandez-Miranda G, Iglesias M, Alameda F, Moreno M, Elisovich C, Eyra E, Real FX, et al. Key contribution of CPEB4-mediated translational control to cancer progression. *Nat Med.* 2012; 18:83–90.
- Pai TP, Chen CC, Lin HH, Chin AL, Lai JS, Lee PT, Tully T, Chiang AS. *Drosophila* ORB protein in two mushroom body output neurons is necessary for long-term memory formation. *Proc Natl Acad Sci USA.* 2013; 110:7898–7903. [PubMed: 23610406]
- Pearson BJ, Eisenhoffer GT, Gurley KA, Rink JC, Miller DE, Sanchez Alvarado A. Formaldehyde-based whole-mount in situ hybridization method for planarians. *Dev Dyn: Off Publ Am Assoc Anat.* 2009; 238:443–450.
- Pique M, Lopez JM, Foissac S, Guigo R, Mendez R. A combinatorial code for CPE-mediated translational control. *Cell.* 2008; 132:434–448. [PubMed: 18267074]
- Richter JD. CPEB: a life in translation. *Trends Biochem Sci.* 2007; 32:279–285. [PubMed: 17481902]
- Rink JC. Stem cell systems and regeneration in planaria. *Dev Genes Evol.* 2013; 223:67–84. [PubMed: 23138344]
- Robb SM, Gotting K, Ross E, Sanchez Alvarado A. SmedGD 2.0: the *Schmidtea mediterranea* genome database. *Genesis.* 2015; 53:535–546. [PubMed: 26138588]
- Robb SM, Ross E, Sanchez Alvarado A. SmedGD: the *Schmidtea mediterranea* genome database. *Nucleic Acids Res.* 2008; 36:D599–606. [PubMed: 17881371]
- Rouhana L, Vieira AP, Roberts-Galbraith RH, Newmark PA. PRMT5 and the role of symmetrical dimethylarginine in chromatoid bodies of planarian stem cells. *Development.* 2012; 139:1083–1094. [PubMed: 22318224]
- Rouhana L, Wang L, Buter N, Kwak JE, Schiltz CA, Gonzalez T, Kelley AE, Landry CF, Wickens M. Vertebrate GLD2 poly(A) polymerases in the germline and the brain. *RNA.* 2005; 11:1117–1130. [PubMed: 15987818]
- Rouhana L, Weiss JA, Forsthoefel DJ, Lee H, King RS, Inoue T, Shibata N, Agata K, Newmark PA. RNA interference by feeding in vitro-synthesized double-stranded RNA to planarians: methodology and dynamics. *Dev Dyn: Off Publ Am Assoc Anat.* 2013; 242:718–730.
- Sanchez Alvarado A, Newmark PA, Robb SM, Juste R. The *Schmidtea mediterranea* database as a molecular resource for studying platyhelminthes, stem cells and regeneration. *Development.* 2002; 129:5659–5665. [PubMed: 12421706]
- Sasaki H, Matsui Y. Epigenetic events in mammalian germ-cell development: reprogramming and beyond. *Nat Rev Genet.* 2008; 9:129–140. [PubMed: 18197165]

- Seydoux G, Braun RE. Pathway to totipotency: lessons from germ cells. *Cell*. 2006; 127:891–904. [PubMed: 17129777]
- Sheets MD, Fox CA, Hunt T, Vande Woude G, Wickens M. The 3′-untranslated regions of c-mos and cyclin mRNAs stimulate translation by regulating cytoplasmic polyadenylation. *Genes Dev*. 1994; 8:926–938. [PubMed: 7926777]
- Shibata N, Rouhana L, Agata K. Cellular and molecular dissection of pluripotent adult somatic stem cells in planarians. *Dev Growth Differ*. 2010; 52:27–41. [PubMed: 20078652]
- Shinn GL. Formation of egg capsules by flatworms (Phylum, Platyhelminthes). *Trans Am Microsc Soc*. 1993; 112:18–34.
- Si K, Giustetto M, Etkin A, Hsu R, Janisiewicz AM, Miniaci MC, Kim JH, Zhu H, Kandel ER. A neuronal isoform of CPEB regulates local protein synthesis and stabilizes synapse-specific long-term facilitation in aplysia. *Cell*. 2003; 115:893–904. [PubMed: 14697206]
- Sievers F, Wilm A, Dineen D, Gibson TJ, Karplus K, Li W, Lopez R, McWilliam H, Remmert M, Soding J, et al. Fast, scalable generation of high-quality protein multiple sequence alignments using Clustal Omega. *Mol Syst Biol*. 2011; 7:539. [PubMed: 21988835]
- Stebbins-Boaz B, Hake LE, Richter JD. CPEB controls the cytoplasmic polyadenylation of cyclin, Cdk2 and c-mos mRNAs and is necessary for oocyte maturation in *Xenopus*. *EMBO J*. 1996; 15:2582–2592. [PubMed: 8665866]
- Steiner JK, Tasaki J, Rouhana L. Germline defects caused by Smed-boule RNA-interference reveal that egg capsule deposition occurs independently of fertilization, ovulation, mating, or the presence of gametes in planarian flatworms. *PLoS Genet*. 2016; 12:e1006030. [PubMed: 27149082]
- Sturm RM, Dowell JA, Li L. Rat brain neuropeptidomics: tissue collection, protease inhibition, neuropeptide extraction, and mass spectrometric analysis. *Methods Mol Biol*. 2010; 615:217–226. [PubMed: 20013212]
- Sudhof TC. Synaptotagmins: why so many? *J Biol Chem*. 2002; 277:7629–7632. [PubMed: 11739399]
- Tan L, Chang JS, Costa A, Schedl P. An autoregulatory feedback loop directs the localized expression of the *Drosophila* CPEB protein Orb in the developing oocyte. *Development*. 2001; 128:1159–1169. [PubMed: 11245581]
- Valpuesta JM, Martin-Benito J, Gomez-Puertas P, Carrascosa JL, Willison KR. Structure and function of a protein folding machine: the eukaryotic cytosolic chaperonin CCT. *FEBS Lett*. 2002; 529:11–16. [PubMed: 12354605]
- Voronina E, Seydoux G, Sassone-Corsi P, Nagamori I. RNA granules in germ cells. *Cold Spring Harb Perspect Biol*. 2011:3.
- Waite, JH. Quinone-tanned scleroproteins. In: Hochachka, PW., editor. *The Mollusca*. Vol. 1. 1983. Metabolic Biochemistry and Molecular Biomechanics. Academic Press; New York, London: p. 467-504.
- Wang J, Gu H, Lin H, Chi T. Essential roles of the chromatin remodeling factor BRG1 in spermatogenesis in mice. *Biol Reprod*. 2012; 86:186. [PubMed: 22495890]
- Wang Y, Stary JM, Wilhelm JE, Newmark PA. A functional genomic screen in planarians identifies novel regulators of germ cell development. *Genes Dev*. 2010; 24:2081–2092. [PubMed: 20844018]
- Wang Y, Zayas RM, Guo T, Newmark PA. *nanos* function is essential for development and regeneration of planarian germ cells. *Proc Natl Acad Sci USA*. 2007; 104:5901–5906. [PubMed: 17376870]
- Wu L, Wells D, Tay J, Mendis D, Abbott MA, Barnitt A, Quinlan E, Heynen A, Fallon JR, Richter JD. CPEB-mediated cytoplasmic polyadenylation and the regulation of experience-dependent translation of alpha-CaMKII mRNA at synapses. *Neuron*. 1998; 21:1129–1139. [PubMed: 9856468]
- Xu S, Hafer N, Agunwamba B, Schedl P. The CPEB protein Orb2 has multiple functions during spermatogenesis in *Drosophila melanogaster*. *PLoS Genet*. 2012; 8:e1003079. [PubMed: 23209437]
- Zayas RM, Hernandez A, Habermann B, Wang Y, Stary JM, Newmark PA. The planarian *Schmidtea mediterranea* as a model for epigenetic germ cell specification: analysis of ESTs from the hermaphroditic strain. *Proc Natl Acad Sci USA*. 2005; 102:18491–18496. [PubMed: 16344473]

Zearfoss NR, Alarcon JM, Trifilieff P, Kandel E, Richter JD. A molecular circuit composed of CPEB-1 and c-Jun controls growth hormone-mediated synaptic plasticity in the mouse hippocampus. *J Neurosci.* 2008; 28:8502–8509. [PubMed: 18716208]

Author Manuscript

Author Manuscript

Author Manuscript

Author Manuscript

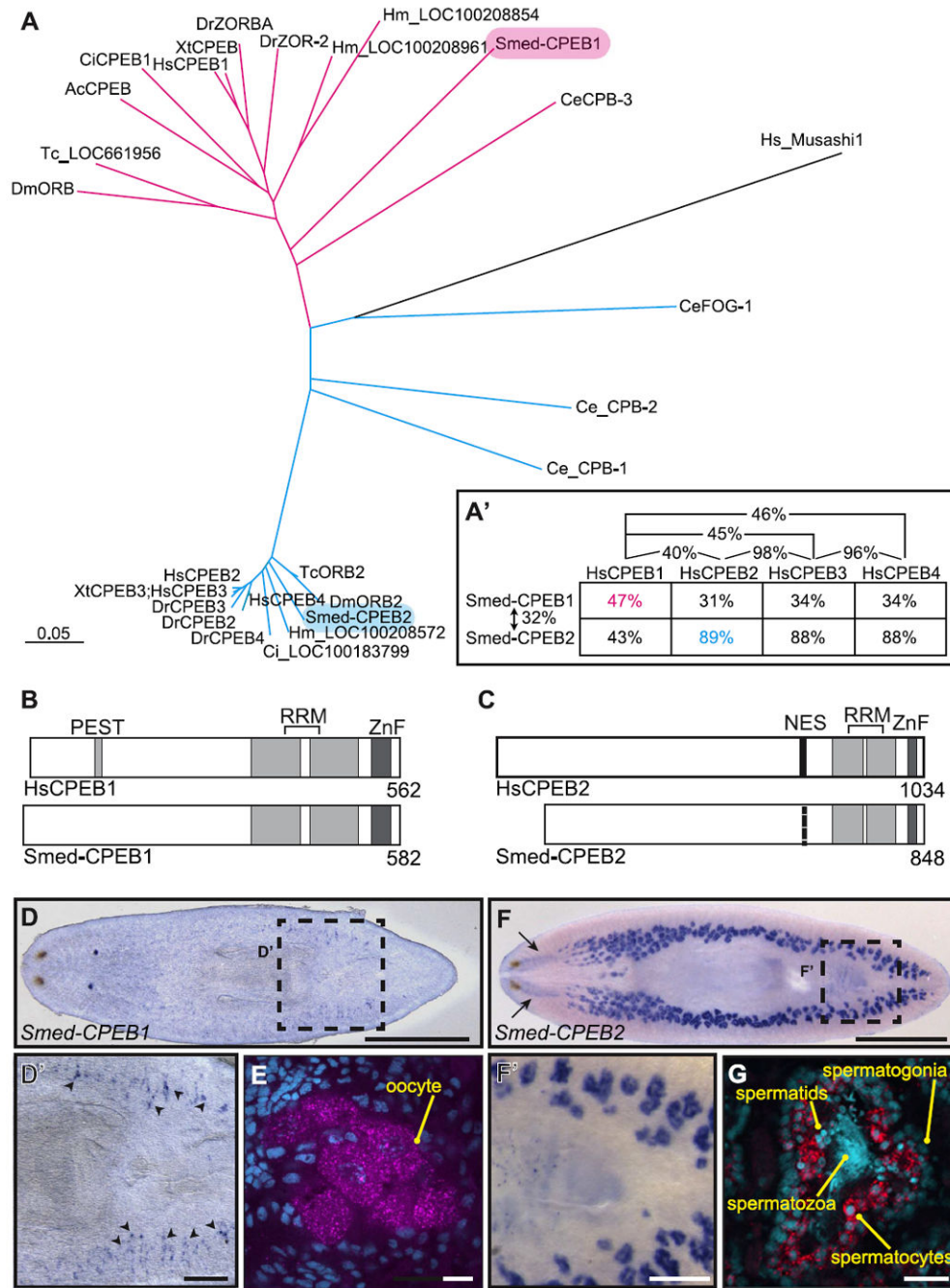


Fig. 1. Expression of CPEB paralogs in sex-specific reproductive structures and central nervous system

(A) Neighbor-joining phylogenetic tree depicting the closer association of Smed-CPEB1 sequence with canonical CPEB subfamily proteins (magenta), and Smed-CPEB2 with members of the CPEB2/3/4 subfamily (blue). Phylogenetic analysis was performed using Clustal Omega under default parameters (Sievers et al., 2011). Abbreviations: *Aplysia californica* (Ac), *Caenorhabditis elegans* (Ce), *Ciona intestinalis* (Ci), *Danio rerio* (Dr), *Drosophila melanogaster* (Dm), *Homo sapiens* (Hs), *Hydra vulgaris* (Hv), *Tribolium castaneum* (Tc), *Schmidtea mediterranea* (Smed), and *Xenopus tropicalis* (Xt). HsMusashi is

included as an outgroup. Scale bar represents 0.05 substitutions per amino acid position. (A') Amino acid sequence identity shared between human and *S. mediterranea* CPEB RNA-binding domains. Highest identities for CPEB1 (pink) and CPEB2 (blue) are shown. (B-C) Human and planarian CPEB1 (B) and CPEB2 (C) protein architecture includes two RNA-recognition motifs (RRM; light gray) and a zinc finger (ZnF; dark gray). A nuclear export signal present in HsCPEB2 (NES; black) is partially conserved in Smed-CPEB2. HsCPEB1 contains a Proline Glutamic Acid Threonine (PEST) domain. (D-G) Wholemount (D, F) and fluorescent (E, G) in situ hybridization reveal expression of *Smed-CPEB1* in ovaries (D) and yolk glands (D') of *S. mediterranea*, whereas *Smed-CPEB2* expression (F) was detected in the brain (arrows) and testes (F'). More specifically, Smed-CPEB1 mRNA was detected in oocytes (E) and *Smed-CPEB2* in spermatogonia and spermatocytes. Scale bars =1 mm (D, F), 0.2 mm (D', F'), and 20 μ m (E, G). Nuclei are stained by DAPI (cyan) in (E) and (G).

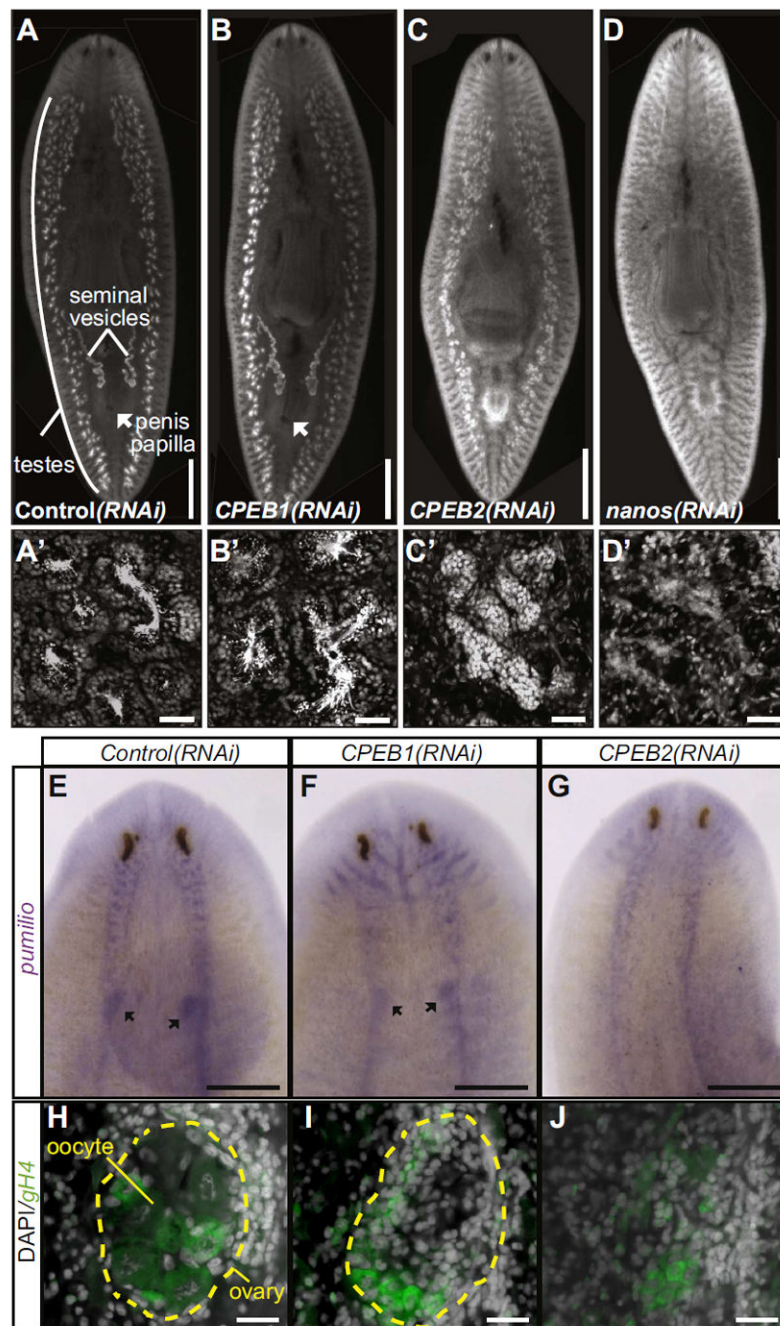


Fig. 2. Smed-CPEB1 is required during oogenesis and Smed-CPEB2 for general maturation of the reproductive system

(A-G) Analysis of reproductive anatomy of samples subjected to two-months of control (A, E), *Smed-CPEB1* (B, F), *Smed-CPEB2* (C, G) or *nanos* (D) RNAi. Abnormalities in development of testes, copulatory complex (penis papilla; white arrow), and accumulation of sperm in seminal vesicles, are apparent by DAPI staining in *CPEB2(RNAi)* (C) and *nanos(RNAi)* (D). Confocal microscopy revealed normal sperm production in control (A') and *CPEB1(RNAi)* (B'), whereas *CPEB2(RNAi)* lacked spermatids and spermatozoa (C').

Testes were not detected in *nanos(RNAi)* (**D'**). (**E-J**) Detection of ovaries by *pumilio* in situ hybridization (ISH) (**E-G**; black arrows) and confocal analysis of DAPI-stained samples (**H-J**; yellow dashed lines) in controls (**E, H**) and *CPEB1(RNAi)* (**F, I**) samples. No ovaries were detected in *CPEB2(RNAi)* by either *pumilio* ISH (**G**) or confocal analysis of DAPI-stained samples (**J**). Oocytes (large cells with condensed chromosomes) present in ovaries of control samples (**H**) were not detected in ovaries of *CPEB1(RNAi)* (**I**). Detection of *Smed-gH4* expression (green; **H-J**) was used as germline stem cell marker. Scale bars =1 mm (**A-D**), 50 μ m (**A'-D'** and **H-J**) and 0.5 mm (**E-G**).

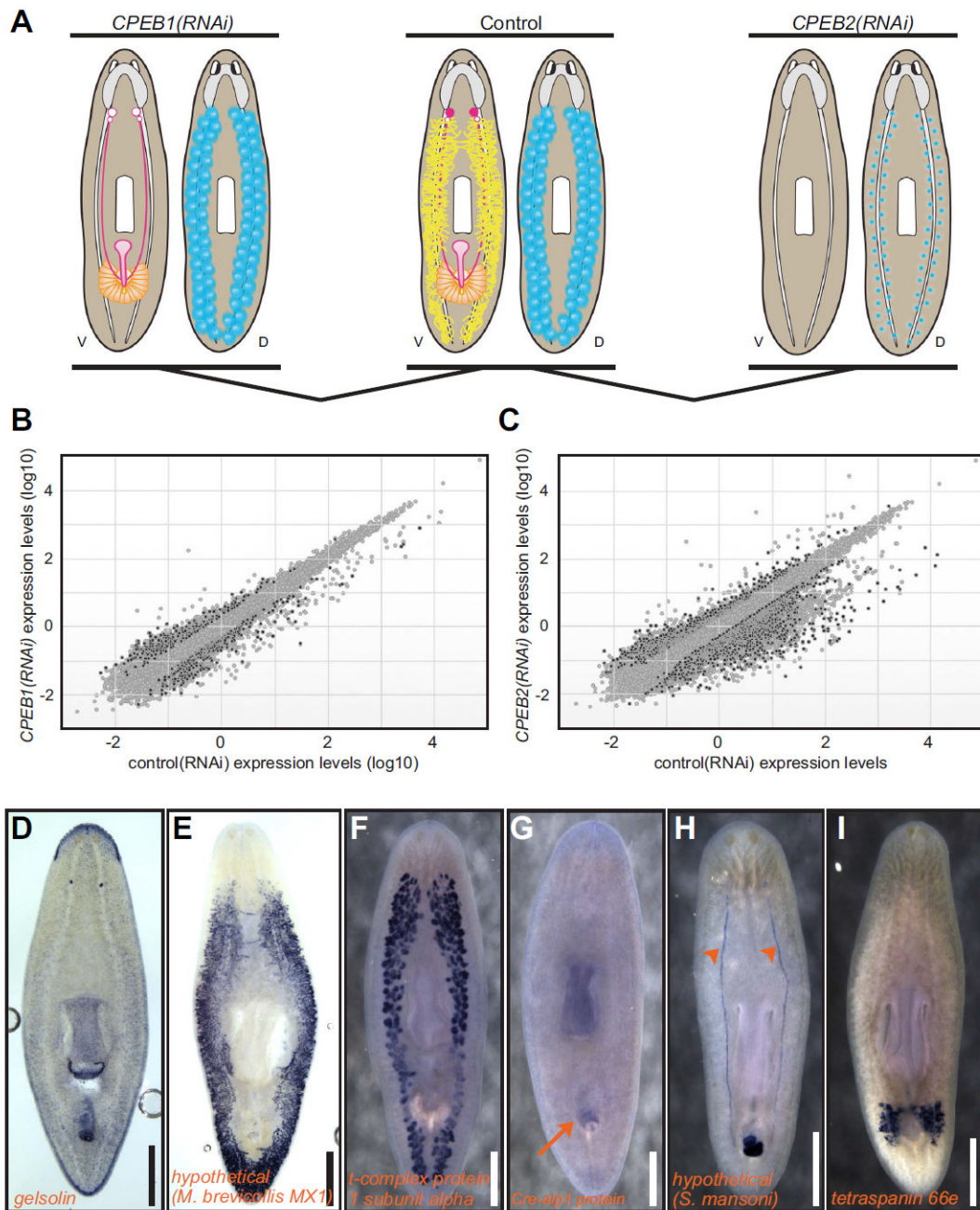


Fig. 3. RNA-seq analysis of *CPEB1(RNAi)* and *CPEB2(RNAi)* uncovers new markers of the planarian reproductive system

(A) Schematic experimental design of RNA-seq analyses highlighting differences between control (middle), *CPEB1(RNAi)* (left), and *CPEB2(RNAi)* reproductive anatomies. Yolk cells (yellow), ovaries (pink circles), ovaries without oocytes (open pink circles), oviducts (pink lines), testes (blue), and copulatory complex (orange glands; pink bursa). Dorsal (D) and ventral (V) views. (B-C) Plots displaying gene expression value means from control(*RNAi*) (*x*-axis) and *CPEB1(RNAi)* (*y*-axis) transcriptomes (B), as well as control(*RNAi*) (*x*-axis) vs. *CPEB2(RNAi)* (*y*-axis) (C). Genes with statistically significant

(p value < 0.05) differences > 2-fold in transcript abundance are indicated (black dots). **(D-I)** WMISH showing markers of reproductive structures identified from RNAseq analysis of *CPEB1(RNAi)* **(D, E)** and *CPEB2(RNAi)* **(F-I)**. Penis papilla (arrow in G) and oviducts (arrowheads in H) are indicated.

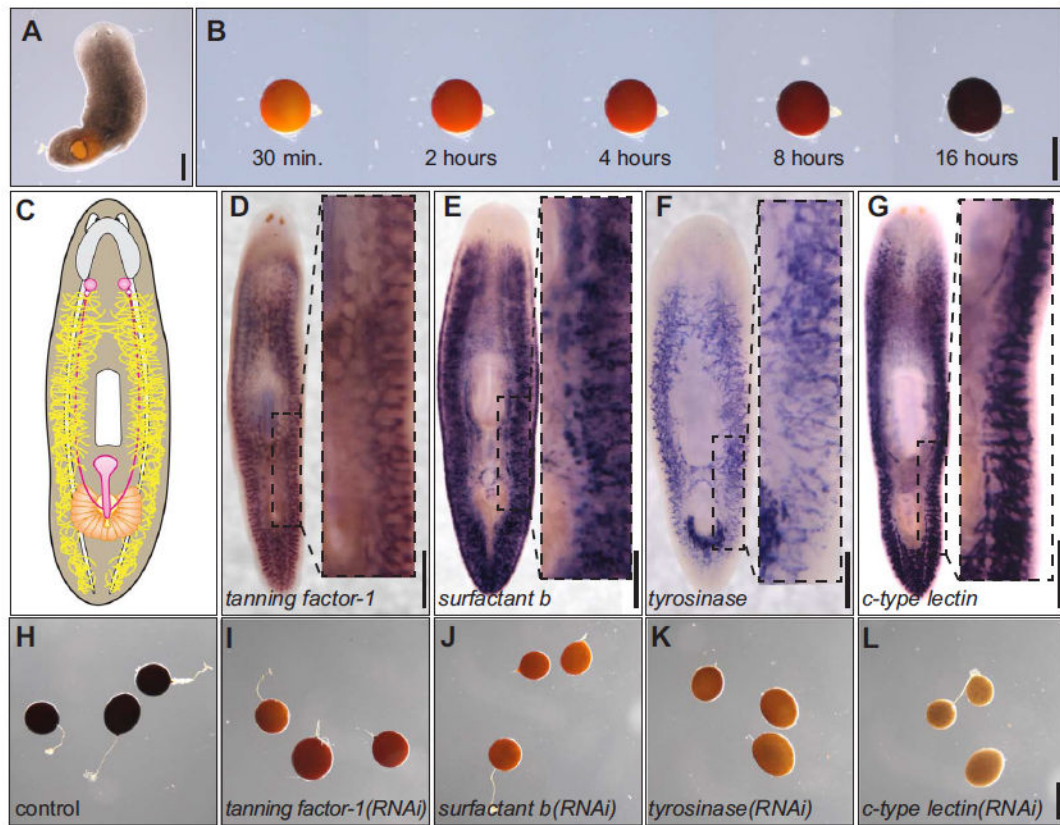


Fig. 4. Genes required for capsule shell maturation and tanning

(A) *S. mediterranea* in the process of capsule deposition. (B) Time-course imaging of capsule tanning process, 0.5–16 h post-deposition. (C) Illustration of female reproductive anatomy with yolk gland distribution represented in yellow. (D–G) Detection of *tanning factor-1* (D), *surfactant b* (E), *tyrosinase* (F), and *c-type lectin* (G) transcripts in yolk glands by WMISH. (H–L) Egg capsules produced by control (H), *tanning factor-1(RNAi)* (I), *surfactant b(RNAi)* (J), *tyrosinase(RNAi)* (K), and *c-type lectin(RNAi)* (L) > 1-month post-deposition. Scale bars=1 mm.

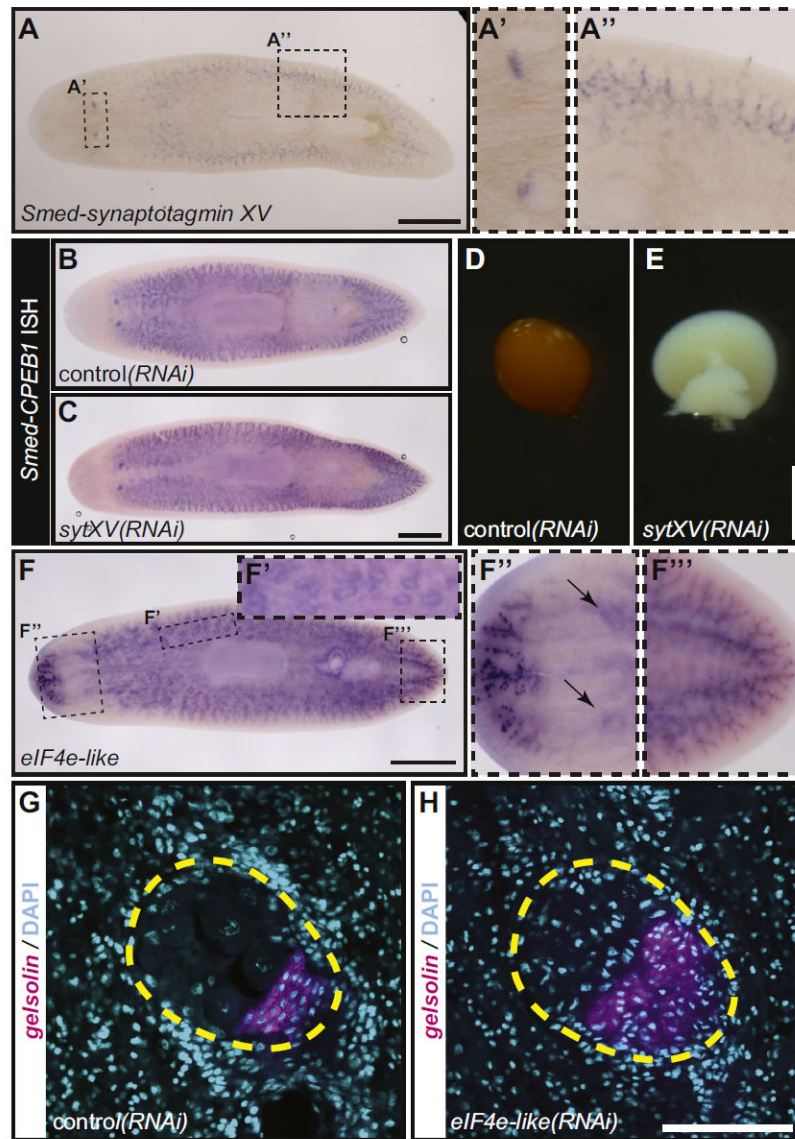


Fig. 5. Identification of genes required for oogenesis and capsule formation
(A) WMISH detects *sytXV* expression in ovaries (**A'**) and yolk glands (**A''**) of *S. mediterranea*. **(B-C)** Assessment of normal oocyte and yolk gland development using *Smed-CPEB1* as a marker in control(*RNAi*) (**B**) and *sytXV(RNAi)* (**C**). **(D-E)** Images of normal capsules produced by control(*RNAi*) (**D**) and shell-less capsules produced by *sytXV(RNAi)* (**E**) captured by dark field microscopy. **(F)** *eIF4e-like* mRNA detection in testes (**F'**), ovaries (arrows; **F''**), and presumably gut goblet cells (**F'''** and **F''''**). **(G-H)** Confocal sections of control (**G**) and *eIF4e-like(RNAi)* (**H**) reveal a decrease in oocyte number (large cells with condensed chromosomes visualized by DAPI (cyan)) and an increase in cells expressing *gelsolin* (magenta) in ovaries (dashed line) of *eIF4e-like(RNAi)* (1.5 vs. 4.7 oocytes/ovary, and 77.0 vs. 25.7 *gelsolin* (+) cells/ovary, of *eIF4e-like(RNAi)* vs. controls, respectively; $p < 0.05$ two-tailed unpaired Student's *t*-test, $n = 3$ biological replicates per group). Scale bars=1 mm (**A-F**) and 100 μ m (**G-H**).

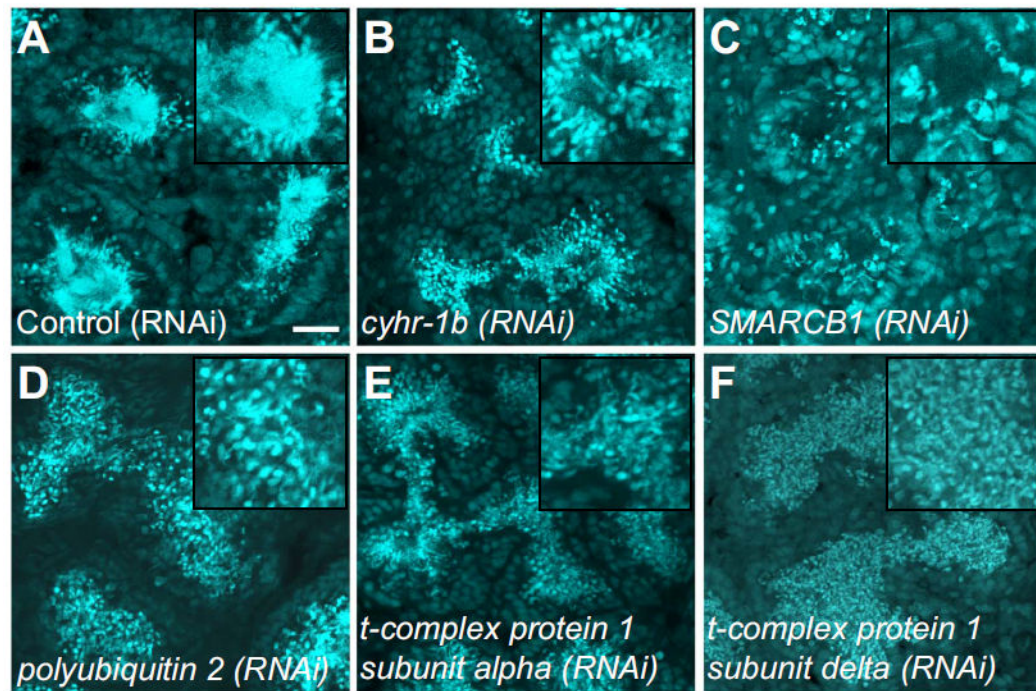


Fig. 6. Genes required for spermatid elongation

Confocal images of testes stained with DAPI from control (A) display normal sperm production and testis morphology, whereas *cyhr-1b* (B), *SMARCB1* (C), *polyubiquitin2* (D), *cct-1* (E), and *cct-4* (F) RNAi lead to spermatid elongation defects. Scale bars=50 μ m.

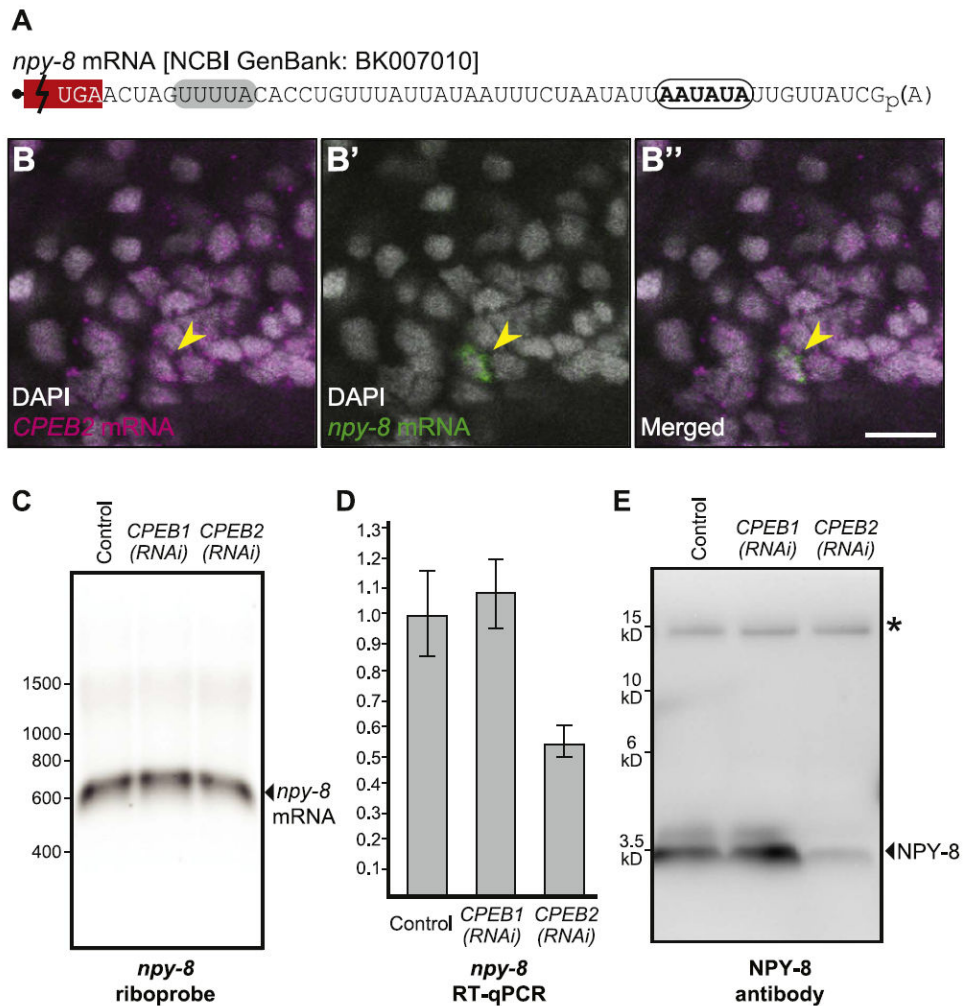


Fig. 7. Neuropeptide Y-8 abundance decreases upon Smed-CPEB2 RNAi
(A) 3' UTR sequence of *npy-8* mRNA (GenBank: BK007010) shows a CPE (gray oval) and potential cleavage and polyadenylation hexanucleotide (white oval). ORF is presented (not to scale; red box) with stop codon. **(B)** Detection of Smed-CPEB2 mRNA (magenta) in neurons expressing *npy-8* (green; **B'**). DAPI-stained nuclei (gray) and position of neuron expressing *npy-8* (arrowhead) are shown. **(B'')** Merged image. Scale bar=20 μ m. **(C)** Northern blot analysis of *npy-8* mRNA in total RNA extracts of control, *CPEB1(RNAi)*, and *CPEB2(RNAi)*. DNA size markers shown in left. **(D)** RT-qPCR analysis of *npy-8* mRNA in total RNA from biological triplicates of control, *CPEB1(RNAi)*, and *CPEB2(RNAi)* normalized to *β -tubulin* mRNA. **(E)** Western blot analysis of NPY-8 neuropeptide in protein extracts of control, *CPEB1(RNAi)*, and *CPEB2(RNAi)*. Position of size markers is shown. Non-specific 15 kD signal (asterisk) serves as endogenous loading control.